EUROPEAN FUSION DEVELOPMENT AGREEMENT

EFDA–JET–PR(04)58

D.Testa, C.Boswell, A.Fasoli, and JET EFDA contributors

Experimental Study of the Dependence of the Damping Rate of n=1 TAEs on the on-axis Safety Factor and Toroidal Rotation Shear

Experimental Study of the Dependence of the Damping rate of n=1 TAEs on the on-axis Safety Factor and Toroidal Rotation Shear

D.Testa[1], C.Boswell[2], A.Fasoli[1,2], and JET EFDA contributors*

[1]CRPP, Association EURATOM – Confédération Suisse, EPFL, Lausanne, Switzerland
[2]Plasma Science and Fusion Center, Massachusetts Institute of Technology, Boston, USA
** See annex of J. Pamela et al, "Overview of Recent JET Results and Future Perspectives", Fusion Energy 2002 (Proc.19 th IAEA Fusion Energy Conference, Lyon (2002).*

Preprint of Paper to be submitted for publication in
Nuclear Fusion

ABSTRACT.

The dependence of the measured damping rate (γ/ω) upon the value of the safety factor on axis (q_0) and of the toroidal rotation shear has been experimentally determined for n=1 Toroidal Alfvén Eigenmodes (TAEs) in JET limiter plasmas with a monotonic safety factor profile and low edge magnetic shear. For $q_0<1$ the n=1 TAE damping rate can reach values up to $\gamma/\omega>8\%$, whereas for $q_0>1.1$ $\gamma/\omega<2\%$ for similar experimental conditions. The transition between these two regimes provides an empirical indication of a possible role of the sawteeth in redistributing the plasma current, hence affecting the damping of low-n TAEs through a different magnetic shear profile. The value of the toroidal rotation shear affects the n=1 TAE damping rate only at high Neutral Beam Injection power (P_{NBI}): for $P_{NBI}>6.5$MW we find that $\gamma/\omega>2\%$ in plasmas with higher rotation shear, whereas for lower P_{NBI} we do not observe any appreciable effect of the rotation shear on γ/ω. These observations indicate that different damping mechanisms for low-n TAEs may be active at low and high performance, prompting further detailed theoretical modelling.

1. INTRODUCTION.

Controlling the interaction between fusion generated α's and modes in the Alfvén frequency range is a crucial issue for the operation of experimental reactors in the burning plasma regime, such as ITER, as these modes can be driven unstable by the slowing-down α's up to amplitudes at which they could cause rapid radial transport of the α's themselves. The need to avoid strongly unstable regimes for some classes of Alfvén Eigenmodes (AEs) can therefore provide additional constraints for the reactor operation regime. On the other hand, if adequate actuators are identified, AEs could be used to affect the thermonuclear plasma burn in a controlled way [1].

Two classes of investigations are conducted on JET: the direct observation of the AE stability limits in the presence of fast particles that can resonate with the modes, and the measurement of the mode damping rate as a function of various plasma parameters, in order to quantify the mechanisms that provide background damping for the AEs in different operating regimes. Results from the first class of studies have been recently reported in Refs.[2,3], thus in this paper we focus on the latter studies. One of the main purposes of the AEs studies on JET is to validate the existing theoretical models and identify the dominant damping mechanisms for global AEs, with the aim of improving the accuracy in the predictions for future burning plasma experiments such as ITER. This approach has characterised the AE active excitation experiments in JET over the last ten years, using the saddle coils as an AE active antenna. The last experimental campaigns aimed at completing the database of damping rate (γ/ω) measurements for AEs with low toroidal mode numbers (n) before the removal of the saddle coils, which occurred during the second half of 2004. A new antenna system [4] is currently being installed on JET to continue along the same lines, but extending the accessible range of toroidal mode numbers to higher values, up to $n\approx 10\div 15$, of more direct relevance to ITER.

In this paper we report our experimental investigation of the role of the safety factor q(r) on axis (q_0) and of the volume-averaged toroidal rotation shear $s_{ROT}=\langle (r/f_{ROT})(df_{ROT}/dr)\rangle$ on the damping rate of global n=1 TAEs in plasmas with a monotonic q-profile.

The strong increase of γ/ω for the saddle coil driven, stable low-n AEs at high edge elongation (κ_{95}>1.5) and triangularity (δ_{95}>0.35) [5] makes it difficult to measure the damping rate for n=1 TAEs in such configurations. Hence our experimental work has mainly focused on plasmas with low κ_{95} and δ_{95}, so as to infer in detail the contribution of additional damping mechanisms in regimes much closer to the marginal stability limit for low-n AEs.

This paper is organised as follows. Section 2 reports the measurement of the dependence of the damping rate of radially extended n=1 Toroidal AEs (TAEs) on q_0. In section 3 we show our measurement of the dependence of γ/ω on s_{ROT}. Finally, Section 4 summarises our conclusions and presents an outlook for future experimental and theoretical studies.

2. EFFECT OF THE VALUE OF THE SAFETY FACTOR ON AXIS ON THE DAMPING RATE OF GLOBAL N=1 TAES.

Theoretical modelling and direct measurements clearly indicate that the safety factor profile has a fundamental role in determining the onset of different classes of global AEs. As an example, the transition from a monotonic q-profile with q_0<1 to a moderately reversed q-profile with q_0>2 corresponds to the transition between fast ion driven "standard" AEs and Alfvén Cascades for otherwise similar fast ion distributions [6]. The role of the magnetic shear s=(r/q)(dq/dr) at the plasma edge (s_{95}) in determining the AE stability has also been demonstrated theoretically [7] and experimentally [8]. Similarly, earlier experimental studies [8] have shown that weakly damped (γ/ω<0.2%) low-n (n=0÷2) modes exist in the AE frequency range in plasmas with a reversed safety factor profile even in the presence of a large edge magnetic shear, contrary to the observations for the monotonic q-profile case, where γ/ω>5% for similar values of s_{95}. These low-n modes observed with a non-monotonic q-profile could be related to the predicted Drift Kinetic AEs [9], but further detailed theoretical modelling is still needed to reach a clear identification.

In this work we focus our attention to the theoretically clearer case of plasmas with a monotonic qprofile. A typical example of the operating scenario considered here is given in Fig.1, where the main plasma parameters are shown for the ohmic JET Pulse No: 52835, for which Fig.2 shows the measurement of the n=1 TAE mode frequency and damping rate. In this discharge the transition to the X-point phase occurs around t=12sec, clearly evident from the increase in the edge triangularity and elongation, and corresponds to a three-fold increase in γ/ω. The mode frequency and damping rate are measured using synchronous detection of the saddle coil driven perturbation [10]. Hence the error bar on the measurement of the mode frequency is very low, not exceeding ≈100Hz, and the relative error on γ/ω is typically of the order of <20% for the cases considered in this work.

Using the saddle coil measurements of the mode frequency and damping rate for n=1 TAEs in ohmic limiter plasmas with a monotonic q-profile, we have constructed a database which contains more than 1500 points, with q_0 in the range 0.76<q_0<1.59. This database covers a wide range in the main plasma parameters (edge elongation and triangularity 1.24<κ_{95}<1.55 and 0<δ_{95}<0.25; central electron density and temperature 1.35<$n_{e0}(10^{19}m^{-3})$<4.2 and 1.1<T_{e0}(keV)<5.6; edge safety factor

$2.5<q_{95}<4.75$), hence represents a significant statistical overview of the damping rate measurements in this configuration. The q-profile is reconstructed by the EFIT code [11] using edge magnetic and internal polarimetry measurements. For the cases considered here of monotonic q-profile, its typical accuracy is estimated to be of the order of 10%. Furthermore, for the cases of $q_0<1$, there is also a very good agreement between the position of the q=1 surface as determined by EFIT and from the sawtooth inversion radius, with the two estimates differing typically by no more than 3÷5cm.

Figure 3 shows the dependence of the measured damping rate for n=1 TAEs on q_0. Considering ohmic plasmas with $\kappa_{95}<1.5$ and $\delta_{95}<0.3$, we find that for $q_0>1.1$ the damping rate of n=1 TAEs does not exceed the value $\gamma/\omega \approx 2\%$ for a variety of electron temperature and density profiles and for different values of the plasma current and magnetic field. On the other hand, we find that in similar experimental conditions γ/ω can reach values up to $\gamma/\omega \approx 8\%$ with $q_0<0.9$. Such observations indicate that very large values of the damping rate ($\gamma/\omega>2\%$) can only be obtained for $q_0<1$ in plasmas with a low magnetic shear, which are then less prone to becoming TAE-unstable than similar plasmas with $q_0>1.1$. Detailed theoretical modelling is necessary to reproduce and provide an interpretation for this phenomenon. The transition between these two regimes, observed for $q_0\approx0.9\div1.1$, is suggestive of a role for the q=1 surface and possibly for the sawteeth, for example an average effect of the sawteeth redistribution of the plasma current providing, on average, a lower magnetic shear in the plasma core, hence favouring core damping via mode conversion [7].

The mode structure of some of the modes detected by the saddle coils was modelled using the set of ideal and resistive MHD codes HELENA [12], CSMISH [13], MISHKA-1 [14] and CASTOR [15]. CSMISH calculates the continuum frequencies for a shaped equilibrium with arbitrary profiles of density, pressure and q. MISHKA-1 is an ideal MHD normal-mode analysis code used to determine the TAE radial and poloidal mode structure, neglecting the plasma compressibility and the coupling to the ion sound wave, whose frequency is typically well below the TAE frequency. CASTOR is a resistive MHD normal-mode analysis code that is used to calculate the continuum damping [16] for the observed modes. CASTOR does not take into account kinetic effects, thus cannot determine the damping due to ion and electron Landau damping.

Figure 4 shows the n=1 continuum calculated with the CSMISH code as function of the safety factor on axis, for values of q_0 in the range $q_0=0.77$ (Fig.4(a)) to $q_0=1.59$ (Fig.4(h)): note that all the pulses considered here have a very similar magnetic shear profile $s(r)=(r/q)(dq/dr)$. Figure 5 shows the mode structure of the n=1 TAE calculated with the MISHKA-1 code as function of the safety factor on axis, $q_0=0.77$ (Fig.5(a)) to $q_0=1.59$ (Fig.5(h)), for the same pulses and time slices of Fig.4. There are two points to note about the Alfvén continuum spectrum for n=1 modes as the value of q0 is increased. First, the gap in the continuum associated with the m=1/m=2 degeneracy moves towards the magnetic axis as the location of the q=1.5 surface moves inwards. In particular, for $q_0>1.5$ the m=1 harmonic is negligible, and the m=4,5 harmonics become the dominant ones for $\sqrt{\psi_N}\approx(r/a)>0.7$. Here ψ_N is the normalised poloidal flux, r is the radial coordinate, and a is the minor radius. Second, the width of the gap at this location decreases. These effects are both expected and have been shown

previously in Ref.[17]. The higher values of q_0 (hence q_{95}) introduce a larger number of poloidal harmonics at the plasma edge, clearly breaking up the TAE gap into a sequence of smaller sub-gaps. Although the n=1 TAEs are global modes extending across the entire plasma, as the value of q_0 is increased the peak in the radial mode structure shifts from being near the edge at low q_0 to tracking the q=1.5 surface. Once q_0>1.5, the gap in the continuum associated with the m=1/m=2 harmonics is no longer in the plasma and the radial mode structure returns to being similar to the lower q_0 structure with the lowest substantial poloidal component being now the m=2 component instead of the m=1. As the value of q_0 is raised, the position of the poloidal harmonics with the larger amplitudes is scanned from the higher to the lower magnetic shear region.

Figure 6a shows the comparison between the measured and computed (using the CASTOR code) mode frequency. The calculated values are within 20% of the measured ones, as already found in previous studies [18]. The variation in the calculated mode frequency with respect to the measured values may be associated to the details of the density profile. There is a much better agreement for the TAEs which are more localised toward the core (i.e., those at higher q_0), suggesting that this part of the density profile is correct. Conversely, there is a larger deviation in the mode frequency for the TAEs that are localised towards the plasma edge (i.e., those at lower q_0). This suggests that the nominal edge density profile used in the CASTOR calculation may not be entirely accurate. The measured density profile (from the Thomson scattering diagnostic) is first mapped onto the poloidal flux surfaces using the equilibrium obtained from EFIT. The density measurements are equally spaced along the major radius and, when mapped to poloidal flux surfaces, have a higher resolution in the core than near the edge of the plasma. This profile is fitted as a fourth order polynomial, and it is this fitted profile which is used by CASTOR. Hence the mode frequency of low-n TAEs that are more edge localised is correspondingly more sensitive to the exact details of the edge density profiles, for which the resolution of the raw measurement and/or the mapping/ fitting procedure may not be sufficiently accurate.

Figure 6b shows the comparison between the measured and computed (using the CASTOR code) damping rate due to the interaction with the continuum. The continuum damping rate γ/ω_{CONT} as calculated by CASTOR has here, as its primary contribution, the interaction of the eigenmode with the continuum at the plasma edge, except for two of the cases ($q_0 \approx 1.6$ and $q_0 \approx 0.75$). Figure 7 shows the results of various CASTOR runs for a m/n=2/1 TAE using the same nominal density profile and plasma shape (low elongation κ_{95}=1.37 and low triangularity δ_{95}=0.06) for various q-profiles obtained at fixed q-shape simply by scaling the value of q_0 in the range $0.75<q_0<1.45$. For this particular choice of density profile, the main interaction with the continuum is initially only at the plasma edge for q_0<1.3. By increasing q_0 the mode structure shifts towards the magnetic axis, and γ/ω_{CONT} decreases as function of q_0 up to q_0=1.35 due to an even lower interaction with the edge continuum. For q_0>1.35 the mode starts interacting with the continuum in the plasma core, hence γ/ω_{CONT} dramatically increases. Note that for q_0>1.5 the m/n=2/1 TAE disappears and the m/n=3/2 becomes the dominant mode. These modelling results are not consistent with the measurements shown in

Fig.3 for low κ_{95} and low δ_{95}, which clearly indicate two different regimes for γ/ω below and above the value $q_0 \approx 0.9 \div 1.1$. We also note in Fig.6(b) and Fig.7 the large difference between the measured g/w and the calculated γ/ω_{CONT}, the two being rather unrelated with no apparent constant scaling factor. Following the same reasoning applied to the calculated mode frequency, in the cases where the calculated damping comes primarily from the interaction with the edge continuum, the edge density profile has an even more significant effect on the absolute value of the continuum damping. On one hand, the very strong dependence of γ/ω_{CONT} on the edge density profile makes it difficult to perform a direct comparison between the damping rate as calculated by CASTOR and the experimental values without measurements of the edge density profile with a spatial resolution much higher than those currently available in JET. On the other hand, even for cases where γ/ω_{CONT} is primarily due to interaction with the continuum in the plasma core, where the measured density profiles are considered to be much more accurate, the continuum damping is considerably below the measured damping. This clearly suggests that the variation of γ/ω a function of q_0 shown in Fig.3 cannot be explained entirely by continuum damping.

3. EFFECT OF THE PLASMA ROTATION AND ITS SHEAR ON THE DAMPING RATE OF GLOBAL N=1 TAES.

Theoretical modelling and direct measurements indicate that low-n AEs have a global structure, i.e., have a radial profile extending over a large fraction of the plasma cross-section. The shear in the toroidal rotation f_{ROT} of the whole plasma column, $s_{ROT}=(r/f_{ROT})(df_{ROT}/dr)$, can thus be expected to have an impact over the effective mode damping. A fluid calculation of the effect of the toroidal rotation profile on the TAE mode frequency in the plasma rest frame shows that:

$$\omega_{TAE} = k_{\|TAE}\langle V_A\rangle\left[1-\left\langle\left(\frac{V_{ROT}}{V_A}\right)^2\right\rangle\right]\cdot . \qquad (1)$$

Considering now the previous experimental results of JT-60U [19], we can take the ansatz:

$$q_{TAE} = \frac{2m+1}{2n} + \frac{1}{2n}\left\langle\frac{V_{ROT}}{V_A}\right\rangle = q_{TAE,0} + \Delta q_{TAE}\,, \qquad (2a)$$

$$k_{\|TAE} = \frac{m+nq_{TAE}}{q_{TAE}R_{TAE}} \approx k_{\|TAE,0} - \frac{1}{R_{TAE}}\frac{2mn}{(2m+1)^2}\left\langle\frac{V_{ROT}}{V_A}\right\rangle\cdot . \qquad (2b)$$

Here R_{TAE} is the position of the (m,m+1)/n TAE gap, V_A is the Alfvén speed, $q_{TAE,0}=(2m+1)/2n$, $k_{\|TAE,0}=(m+nq_{TAE,0})/R_{TAE}/q_{TAE,0}$ and $\Delta q_{TAE}=\langle V_{ROT}/V_A\rangle/2n$, where the brackets indicate

averaging over the eigenfunction profile. Now combining Eqs.(2(a), 2(b)) into Eq.(1) we note that that the lowest order correction to $\omega_{TAE} \propto (\langle V_{ROT}/V_A \rangle)^p$, with p=1,2,…, comes from the $q_{TAE}=q_{TAE,0}+\Delta q_{TAE}$ term, with $\Delta q_{TAE} \propto \langle V_{ROT}/V_A \rangle$. This then leads to a linear correction of the TAE frequency in the plasma rest frame (i.e., without Doppler shift) as function of the toroidal plasma rotation:

$$\omega_{TAE}=k_{\|TAE,0}\left\langle V_A\right\rangle\left[1-\frac{2m}{(2m+1)(4m+1)}\left\langle\frac{V_{ROT}}{V_A}\right\rangle\right] . \quad . \qquad (3)$$

The result of Eq.(3) $\omega_{TAE} \approx \omega_{TAE,0}$-const*$\langle V_{ROT}/V_A \rangle$ was obtained in the limit $V_{ROT}/V_A=o(\varepsilon)$, which is the typical case in JET since $V_{ROT} \approx 5.5\times10^4$m/s whereas $V_A \approx 4.5\times10^6$m/s. The correction to the TAE mode frequency in the plasma rest frame can thus be neglected: considering the reference case of a m/n=2/1 TAE, we have that $\Delta\omega_{TAE}/\omega_{TAE} \approx 0.1\times\langle V_{ROT}/V_A \rangle \approx 1.3\times10^{-3}$. This also indicates that the standard fluid codes (such as CSMISH, MISHKA-1 and CASTOR) that do not consider the plasma rotation can be used to calculate the TAE radial structure. On the other hand, it is possible that the shear in the toroidal rotation over the eigenfunction profile may affect the TAE damping rate. This can be evaluated experimentally, as reported here. Theoretically, only ad-hoc codes that consider explicitly the toroidal rotation profile would provide a meaningful result [20], but such codes are not yet routinely applicable to JET data.

A typical example of the operating scenario considered here for the toroidal rotation scan is given in Fig.8, where the main plasma parameters are shown for the JET Pulse No: 52835: f_{ROT} is directly measured using the Doppler shift of the C^{6+} charge-exchange line (5290.54Å). Figure 9 shows the measurement of the n=1 TAE mode frequency and damping rate for this discharge during the rampup in the NBI power (P_{NBI}). We note that the ion temperature (T_i) and the normalised plasma beta (β_N) increase together during the P_{NBI} ramp-up with the toroidal rotation frequency, affecting the measured damping rate as previously reported in Ref.[21]. Hence, to separate the role of f_{ROT} and of s_{ROT} from that of T_i, P_{NBI} and β_N, we have constructed a database grouping the γ/ω measurements as function of the number and energy of the individual NBI injector modules (PINI) used for this rotation scan. This database contains more than 450 points in total, and allows us to study the effect of the shear in the toroidal plasma rotation on the n=1 TAE damping rate for otherwise very similar values of the main plasma parameters affecting γ/ω, such as P_{NBI}, β_N, q_0, κ_{95} and δ_{95}. On the other hand, there is still some data scatter for each individual PINI subset in the q_{95}, n_e and T_e values. Figure 10 shows that, when comparing data points with similar level of P_{NBI}, the shear in the plasma rotation has no clear effect on the damping rate of n=1 TAEs for $P_{NBI} \leq 5$MW. Only for $P_{NBI}>6.5$MW can a general trend be identified in the database we collected: the damping rate for n=1 TAEs is always $\gamma/\omega>2\%$ in pulses characterised by a higher s_{ROT}, as shown in Fig.10(b). We note that the transition in γ/ω occurs for $s_{ROT} \approx 0.52 \div 0.55$, with constant edge elongation

$1.38<\kappa_{95}<1.42$ and edge triangularity $0.05<\delta_{95}<0.07$. Moreover, for $s_{ROT}<0.51$ we have that $0.83<q_0<1.16$, $2.55<q_{95}<3.45$, $2.9<T_{i0}(keV)<3.9$, $0.47<\beta_N<0.71$, and for $s_{ROT}>0.56$ we have that $0.82<q_0<1.04$, $2.65<q_{95}<3.2$, $0.54<\beta_N<0.63$ and $3.3<T_{i0}(keV)<3.7$. Hence, there is a very good superposition with no particular clustering of the q, β_N and T_{i0} values as function of s_{ROT} in the subset of the database shown in Fig.10b. Thus we conclude that the scatter in β_N and T_i (as well as that in q_0 and q_{95}) is not sufficient to explain the transition in the measured damping rate as function of s_{ROT} for $P_{NBI}>6.5$MW.

Figure 11 shows the n=1 TAE continuum and radial structure for the low//high s_{ROT} comparison cases as function of P_{NBI}, calculated with the CSMISH and MISHKA-1 codes, respectively. The increase in P_{NBI}, hence T_i and β_N, does not affect the continuum nor the eigenfunction profile, which shows an odd parity in this particular case. This comparison demonstrates that the effect of s_{ROT} on γ/ω for n=1 TAEs as a function of P_{NBI} occurs for modes with very similar eigenfunction profiles, hence excluding empirically the role of the continuum [16] or the radiative [22] damping as a possible cause for the measured trend in γ/ω. These observations suggest also that the damping mechanisms active at low performance are different from those active at high performance, with the former not affected by the shear in the toroidal rotation profile. However, a more quantitative analysis requires the comparison with theoretical models which explicitly include the role of the toroidal rotation and its shear in the calculation of the TAE radial structure and damping rate, such as those considered in Ref.[19] and Ref.[20]. The results reported here are also generally consistent with the stabilisation of fast ion driven low-n radially-localised TAEs for counter-tangential NBI, previously observed in JT-60U plasmas, which was associated with the deformation of the TAE radial structure induced by a sheared toroidal rotation profile [19].

4. CONCLUSION AND AN OUTLOOK: THE NEW JET ANTENNA FOR THE EXCITATION OF HIGH-N AES.

After about ten years of operation, the 2004 JET experimental campaigns have been the last where the saddle coils were used to drive and detect the damping rate of low-n AEs. This experimental work has been useful in providing detailed benchmarks for the theoretical predictions of the TAE stability in ITER, see for instance Refs.[5,7,9,18,21]. In this respect, the measurements reported here of the dependence of γ/ω for n=1 TAEs on the toroidal rotation shear and safety factor on axis represent the logic conclusion of our experimental effort on low-n TAEs.

In this paper we have presented experimental evidence that the value of the safety factor on axis affects the damping rate of n=1 TAE in ohmic limiter discharges. Our measurements indicate that for $q_0>1.1$ the damping rate of n=1 TAEs does not exceed the value $\gamma/\omega\approx2\%$, whereas in the same experimental conditions γ/ω can reach values up to $\gamma/\omega\approx8\%$ with $q_0<0.9$. Hence regimes with $q_0<1$ would appear to be less prone to low-n TAE instabilities. The transition between these two regimes suggests a possible role for the q=1 surface and the sawteeth redistribution of the plasma current, and detailed theoretical modelling is needed to reproduce these observations. The measurement of

the different effect of the shear in the toroidal rotation profile on the damping rate of n=1 TAEs as function of P_{NBI} provides empirical indications that different damping mechanisms are active at low and high performance. Similarly to the q_0-scan case, detailed theoretical modelling using codes that include explicitly the sheared toroidal rotation profile is needed to reproduce these observations. Such lack of detailed comparison between measurements and models leaves some uncertainties on the prediction for the TAE stability in future burning plasma experiments such as ITER. A detailed comparison work should start from the large database of low-n TAE data that we have collected so far, of which the data presented in this paper are a typical example. At the same time, the design and installation of the new high-n TAE antennas [4] for JET represent the logic step forward towards a more detailed benchmarking of the existing models for high-n AEs in ITER regimes.

ACKNOWLEDGEMENTS.

The authors would like to acknowledge the contribution of the whole JET experimental team, and in particular G.Giroud and T.Bolzonella for their analysis of the CX and q-profile measurements, and S.Sharapov for his assistance with the MISHKA and CASTOR calculations.

This work has been conducted under the European Fusion Development Agreement. D.Testa and A.Fasoli were partly supported by the Fond National Suisse pour la Recherche Scientifique, Grant 620-062924. C.Boswell was partly supported by the US DoE Contract DE-FG02-99ER54563.

REFERENCES.

[1]. A. Fasoli, *Burning plasma physics: the new frontier of fusion energy science*, Invited Oral, Proceedings EuroScience Open Forum, Stockholm (Sweden), 2004.

[2]. D. Testa et al., Plasma Phys. Control. Fusion **46** (2004), S59.

[3]. D. Testa et al., Paper EX/P4-45, Proceedings 20th IAEA Fusion Energy Conference, Vilamoura (Portugal), 2004.

[4]. A. Fasoli et al., Proceedings 8th IAEA Technical Committee Meeting on Energetic Particles in Magnetic Confinement Systems, San Diego (USA), 2003; D.Testa et al., Proceedings 23rd Symposium on Fusion Technology, Venice (Italy), 2004.

[5]. D. Testa et al., Nucl. Fusion **41** (2001), 809.

[6]. S. Sharapov et al., Phys. Plasmas **9** (2002), 2027; F.Zonca et al. Phys. Plasmas **9** (2002), 4939.

[7]. A. Jaun et al., Plasma Phys. Control. Fusion **43** (2001), A207; A.Jaun et al., Phys. Plasmas **5** (1998), 2952; A.Jaun et al., Nucl. Fusion **40** (2000), 1343; A.Fasoli et al., Phys. Lett. **A265** (2000), 288.

[8]. D. Testa et al., Paper P5.007, Proceedings 28th EPS Conference on Controlled Fusion and Plasma Physics, Madeira (Portugal), 2001; D.Testa et al., Paper P1.021, Proceedings 29th EPS Conference on Controlled Fusion and Plasma Physics, Montreux (Switzerland), 2002.

[9]. A. Jaun et al., Nucl. Fusion **40** (2000), 1343.

[10]. A. Fasoli et al., Phys. Rev. Lett. **75** (1995), 645.

[11]. D. O'Brien et al., Nucl. Fusion **32** (1992), 1351.
[12]. G. Huysmans et al., Proceedings CP90 Conference on Computational Physics (World Scientific Publishing Company 1991), 371.
[13]. G. Huysmans et al., Physics of Plasmas **8** (2001), 4292.
[14]. A. Mikhailovksi et al., Plasma Physics Reports **23** (1997), 844.
[15]. W. Kerner et al., Journal of Computational Physics **142** (1998), 271.
[16]. F. Zonca, L. Chen, Phys. Rev. Lett. **68** (1992), 592.
[17]. H. Holties et al., Phys. Plasmas **4** (1997), 709.
[18]. D. Testa et al., Nucl. Fusion **43** (2003), 479.
[19]. M. Saigusa et al., Nucl. Fusion **37** (1997), 1559.
[20]. B. van der Holst et al., Phys. Rev. Lett.—**84** (2000), 2865; B. van der Holst et al., Phys. Plasmas **7** (2000), 4208.
[21]. D. Testa et al., Nucl. Fusion **43** (2003), 724.
[22]. C. Cheng, Phys. Rep. **211** (1992), 1; G.Fu et al., Phys. Plasmas **3** (1996), 4036.

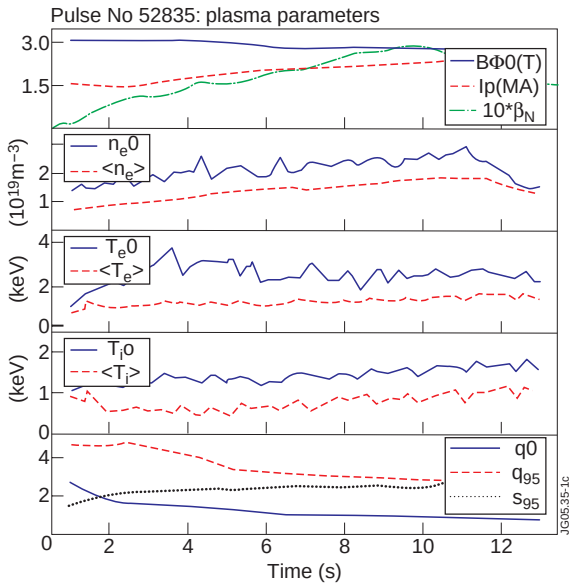

Figure 1: Main plasma parameters of Pulse No: 52835, an example of the typical JET operating scenario with a monotonic q-profile used for the q_0-scan in this work.

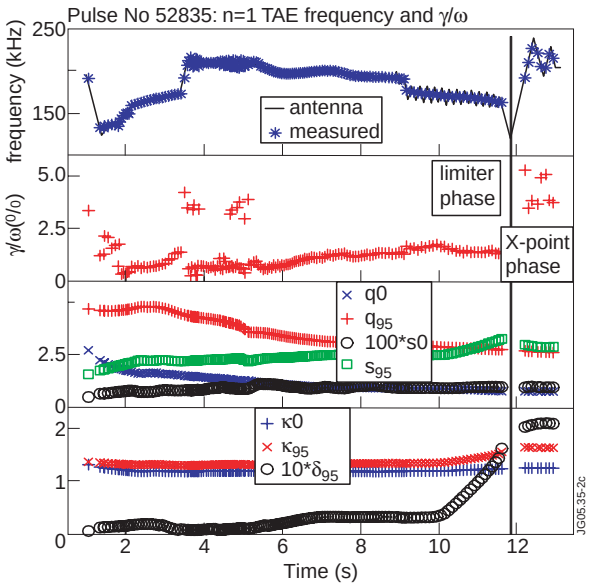

Figure 2: Overview of the damping rate measurements for the reference ohmic Pulse No: 52835. Note the marked increase in γ/ω after the transition to the X-point phase.

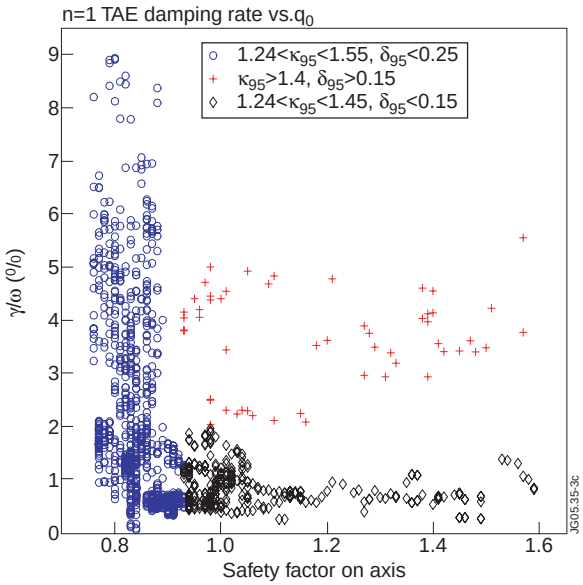

Figure 3: The scaling of the measured damping rate for n=1 TAEs vs.q_0. Note that for q0>0.95, high value of the damping rate γ/ω>2%, can only be obtained at high κ_{95} and δ_{95}.

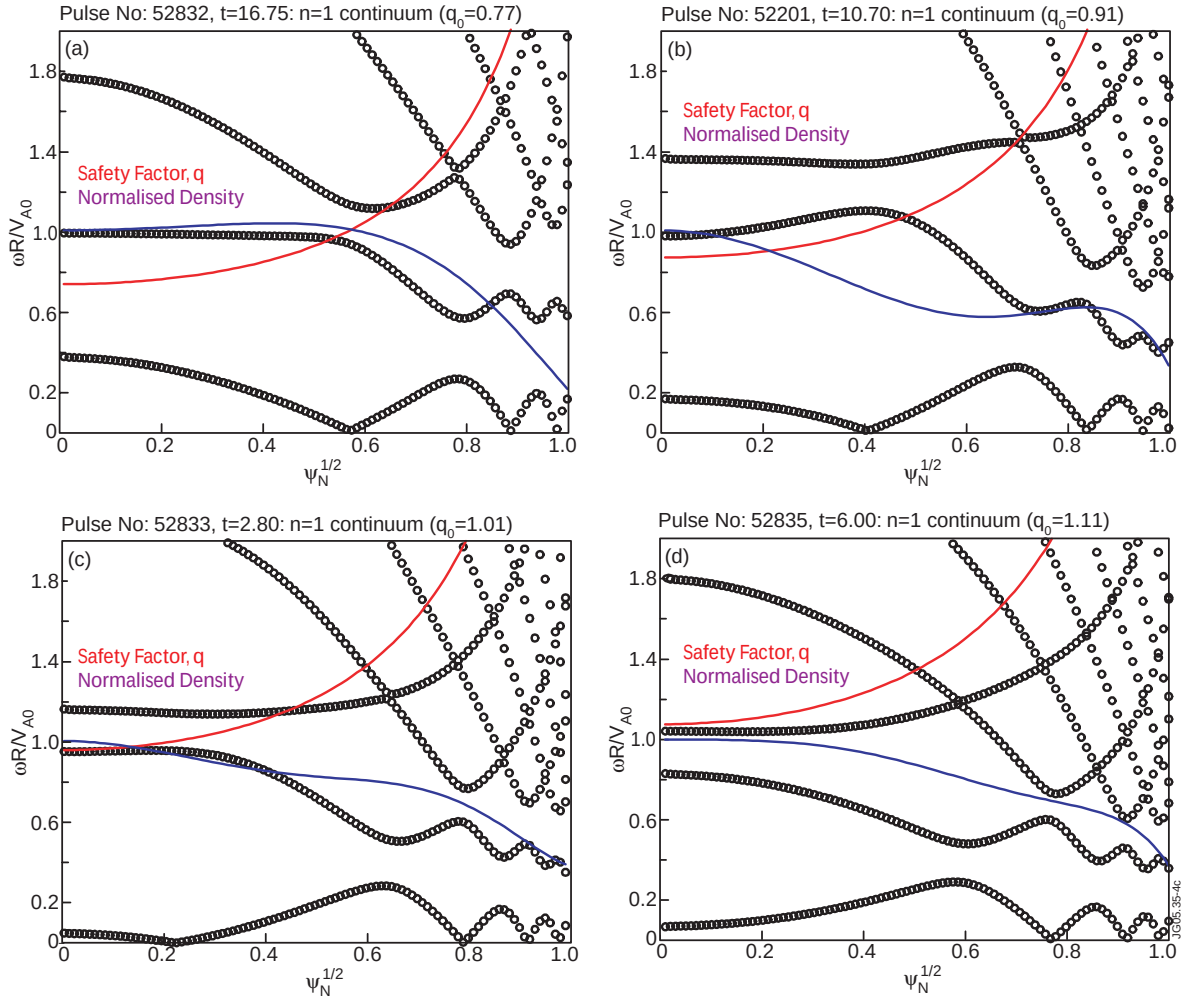

Figure 4: The n=1 continuum calculated with the CSMISH code as function of the safety factor on axis, q_0=0.77 (Fig.4A) to q_0=1.59 (Fig.4H): note that all pulses considered here have a very similar magnetic shear profile s=(r/q)(dq/dr). Here ψ_N is the normalised poloidal flux, with $\sqrt{\psi_N} \approx r/a$.

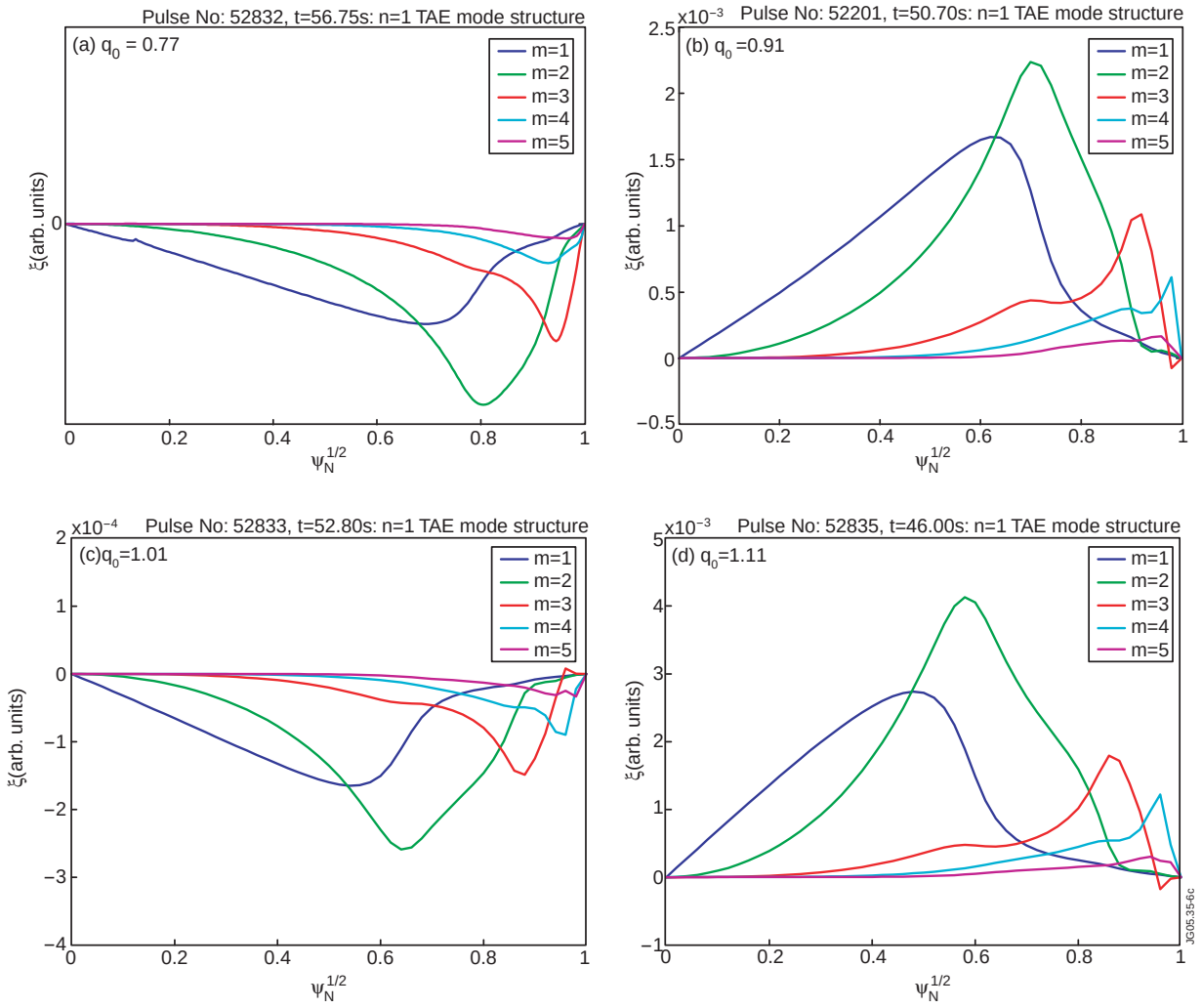

Figure 5: The mode structure of the n=1 TAE calculated with the MISHKA-1 code as function of the safety factor on axis, q_0=0.77 (Fig.5A) to q_0=1.59 (Fig.5H), for the same pulses and time slice of Fig.4. As q_0 increases, the harmonic structure globally shifts towards the magnetic axis.

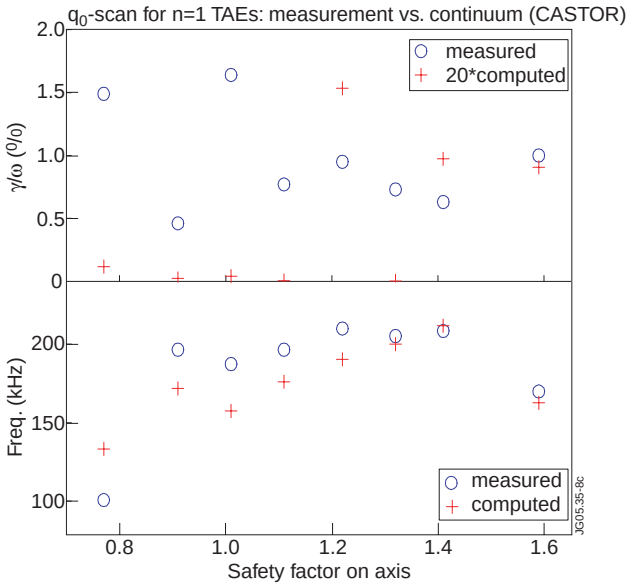

Figure 6: Comparison between the measured and calculated n=1 TAE frequency and damping rate as function of q_0. There is a very good agreement for the mode frequency, but a large difference in γ/ω. Note that the continuum damping calculated by CASTOR is the upper bound for such quantity, particularly when γ/ω_{CONT} is very small (as here), due to difficulties in reaching convergence.

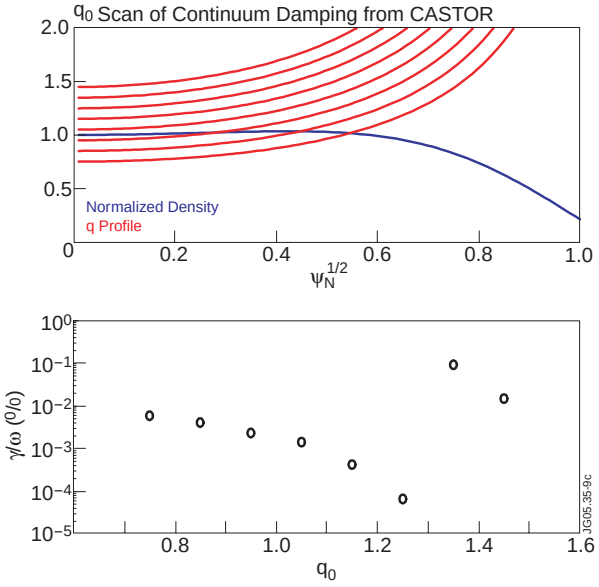

Figure 7: The continuum damping calculated by CASTOR as function of q_0 for the same nominal density profile and edge plasma shape. Note first the reduction and then the increase in γ/ω_{CONT}, which is associated with the shifting of the mode structure towards the magnetic axis and a different interaction with the edge (dominant for q_0<1.3) and core (dominant for q_0>1.3) continuum.

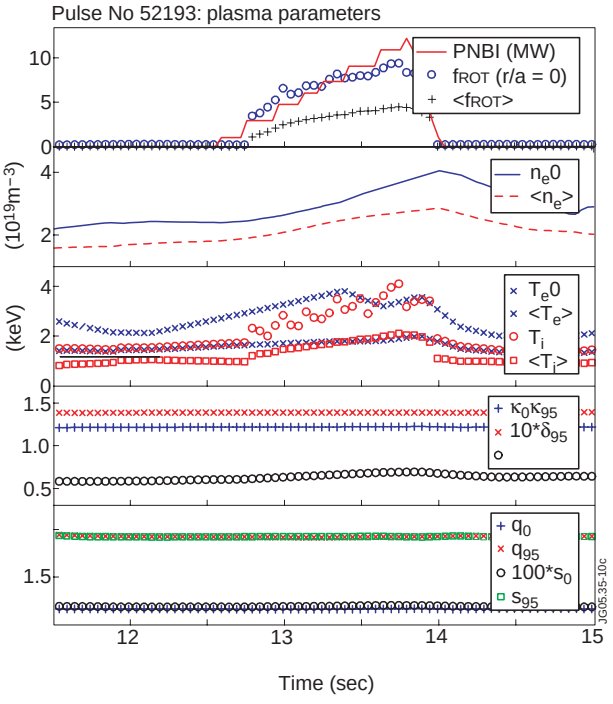

Figure 8: Main plasma parameters of Pulse No: 52193, an example of the typical JET operating scenario with a monotonic q-profile used in this work to study the dependence of γ/ω for n=1 TAEs on the plasma rotation and its shear.

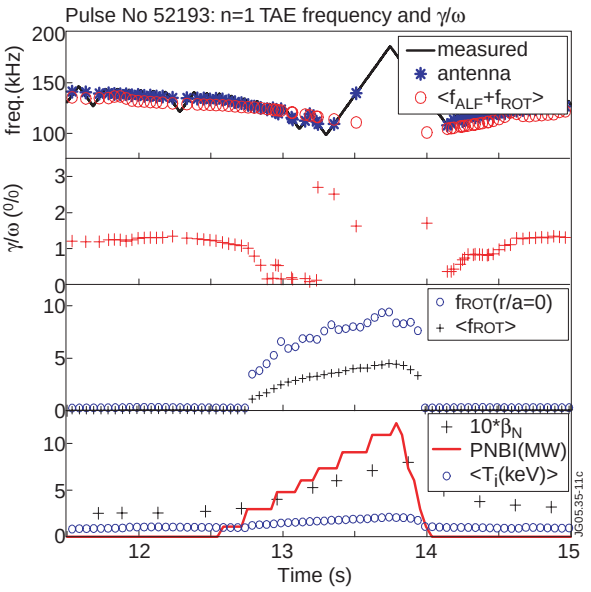

Figure 9: Overview of the damping rate measurements during the P_{NBI} ramp-up in Pulse No: 52193: here $<f_{ALF}+f_{ROT}>$ is the computed volume averaged n=1 TAE frequency including the Doppler shift due to the toroidal rotation. Note the variation of γ/ω as P_{NBI}, $<T_i>$, β_N and f_{ROT} all increase together.

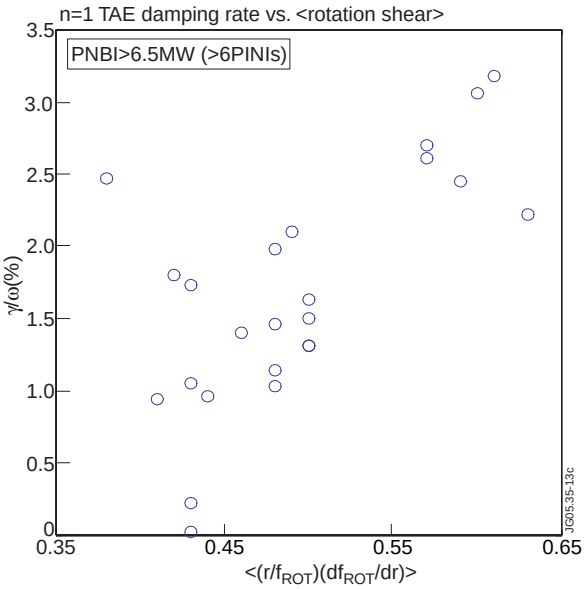

Figure 10b: The dependence of γ/ω for n=1 TAE on the volume-averaged toroidal rotation shear for P_{NBI}>6.5MW. We notice that γ/ω>2% always for s_{ROT}>0.55, indicating that the toroidal rotation shear may play some role in determining the n=1 TAE damping rate at high plasma performance.

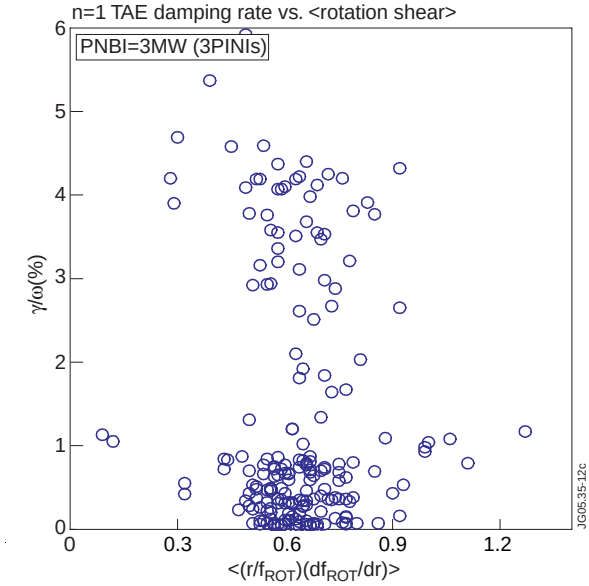

Figure 10a: The dependence of γ/ω for n=1 TAE on the volume-averaged toroidal rotation shear for P_{NBI}=3MW. Notice the large scatter in the data, indicating that $<s_{ROT}>$ plays no role in determining the n=1 TAE damping rate at low plasma performance.

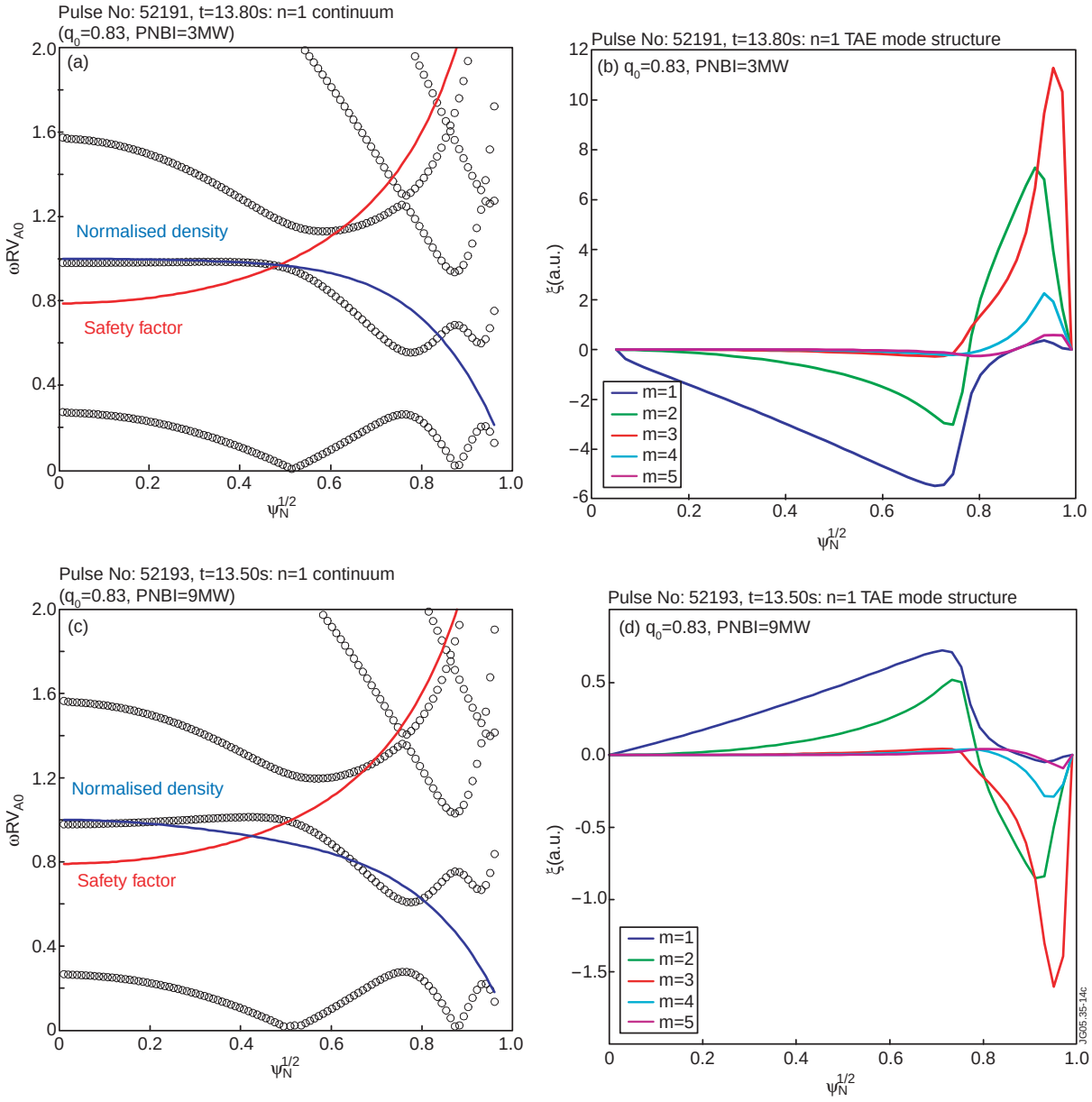

Figure 11: The n=1 TAE continuum and mode radial structure for the low/high rotation shear comparison cases as function of P_{NBI}. Note that the increase in P_{NBI} does not affect the mode radial structure, in this case showing an odd parity.